

喷瓷管道焊接接头的自熔覆防护

陈玉华，王勇，韩涛，董立先

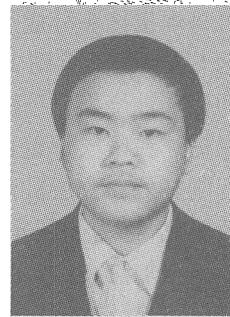
(石油大学 机电学院, 山东 东营 257061)

摘要: 通过分析焊接对喷瓷管道焊接接头处瓷层的影响, 提出了用自熔覆法对焊接接头进行防护。试验结果表明, 在合适的电流下采用 TIG 焊打底能够使焊口附近的瓷层重熔并向焊缝流布、熔覆, 在焊缝区形成保护层, 起到自熔覆防护作用; 焊前管端预涂釉浆能有效增加焊后接头区自熔覆瓷层的厚度, 提高瓷层的防护效果; 焊后采用火焰加热对接头区进行重熔处理, 可以消除瓷层中气泡、裂纹等缺陷。采用焊前管端预涂釉浆、TIG 焊打底、焊条电弧焊填充、焊后接头区瓷层重熔处理等配套措施能够有效解决喷瓷管道焊接接头的防护问题, 焊后不用进行内补口。

关键词: 防腐; 喷瓷管道; 焊接; 接头防护; 自熔覆性能

中图分类号: TG 401 文献标识码: A 文章编号: 0253-360X(2005)02-49-04

陈玉华



0 序言

无机非金属涂层比传统的有机防腐涂层具有更优异的耐蚀、耐磨和耐热性能, 近几年国内外越来越多的学者开始从事在金属基体上制备陶瓷及玻璃涂层的研究^[1~3]。喷瓷管道^[4]是无机非金属涂层在管道防腐上的成功应用。喷瓷管道焊接时, 和所有带内涂层的管道面临着同样的问题——焊接接头的防护问题。目前, 管道接头内防护技术主要有自动补口机法、无焊承插压接法、螺纹连接法、内衬保护套焊接法、记忆合金套法等, 这些方法在管道连接时多数需要对管端加工或强力组装, 对于喷瓷管道不是很适合。另一方面, 现有的焊后内补口技术一般采用有机涂料, 在耐蚀性上与瓷层不匹配, 限制了整条管线的使用寿命。试验中发现, 由于瓷层是耐高温的无机材料, 其软化温度为 600~700 °C, 如果采用合适的焊接工艺瓷层非但不会像有机涂层那样被焊接电弧烧损, 反而会在焊接热作用下软化并向焊缝流动、覆盖焊缝, 焊接完成后在接头区形成覆盖层起保护层的作用, 焊后不用补口。将瓷层在焊接热作用下软化、向焊缝流动、在整个接头区形成完整无缺陷的防护层的性能称为瓷层的自熔覆性能。利用瓷层的自熔覆性能可达到焊后无内补口的目的, 而且接头区与管道内壁均为瓷层防护, 其寿命相当, 提高了整条管线的使用寿命, 这种无内补口的防护方法称为自熔覆防护。

通过对比焊条电弧焊和 TIG 焊两种打底工艺对喷瓷管道焊接接头性能的影响, 确定了 TIG 焊打底的工艺参数。利用瓷层的自熔覆性能, 通过焊前管端预涂釉浆、焊后接头区瓷层重熔处理等方法对喷瓷管道的焊接接头进行了防护, 焊后不用补口即可得性能优良、保护效果良好的接头。

1 试验方法及材料

管道环焊缝的焊接是全位置焊, 在管子最上端(12 点位置)的内瓷层焊接时受到的电弧吹力和熔融瓷层自身的向下的重力都是最大的, 此处瓷层自熔覆能力最差, 若此处能够达到自熔覆防护则整个接头都能自熔覆防护。因此, 采用平板进行背面自熔覆试验模拟该处的情况。平板尺寸为 150 mm × 60 mm × 6 mm, 材料为 Q235。采用热熔覆法在试块上制备瓷层, 熔覆温度为 760 °C, 试验用玻璃釉料成分见表 1。

表 1 玻璃釉料化学成分(质量分数, %)

Table 1 Chemical constitution of frit

Na ₂ O	Al ₂ O ₃	B ₂ O ₃	SiO ₂	MnO ₂	MoO ₃	WO ₃	NiO
22.32	7.08	14.71	31.26	0.11	18.5	5.03	1.0

2 试验结果及分析

2.1 焊条电弧焊热循环对瓷层的影响

目前,在国内外管道施工领域中接口的连接主要是通过电弧焊的方法,而在国内又以焊条电弧焊为主。采用焊条电弧焊焊接喷瓷管道会对管道接头背面的瓷层造成不同程度的破坏,依据瓷层的破坏程度可将焊接接头分成焊缝区 A、瓷层重熔区 B、易脱瓷区 C 三个区(见图 1)。焊缝区由于温度过高,背面的瓷层被烧损,打底焊缝金属裸露在外面,没有瓷层保护。在紧挨焊缝区的外围,由于焊接热作用的温度刚好处在瓷层的软化温度范围内,这里的瓷层重新熔化,称为瓷层重熔区。在瓷层重熔区由于焊接的高温加热,从金属、瓷釉及金属与瓷釉的界面析出气体,焊接热循环的冷却速度快,使气体来不及通过瓷层逸出,从而瓷层与基体金属界面上产生了大量气泡(见图 2),这些气泡大大降低了瓷层的防腐效果。在瓷层重熔区的外围,由于焊接热作用的温度较低瓷层没有软化,产生了较大的热应力致使涂层内部产生裂纹,使得瓷层易脱落,该区称为易脱瓷区(见图 3)。远离易脱瓷区的地方,焊接热对瓷层的影响较小,瓷层基本不发生变化。由此可见,直接采用焊条电弧焊焊接喷瓷管道,焊接接头处瓷层已遭不同程度的破坏,不能起到防护作用,需要进行焊后内补口。

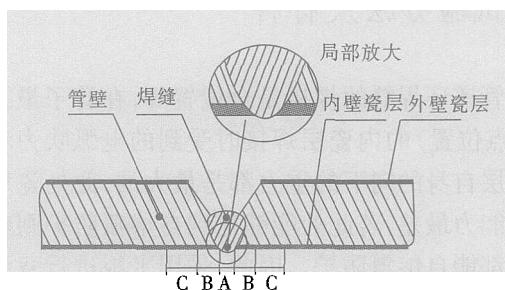


图 1 喷瓷管道焊接接头示意图

Fig. 1 Welded joints of sprayed porcelain pipe

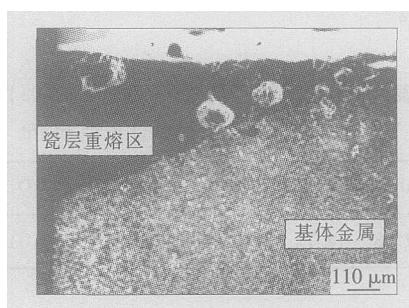


图 2 焊后重熔区气泡形貌(SEM)

Fig. 2 Morphology of air bubbles in remelting area after welding

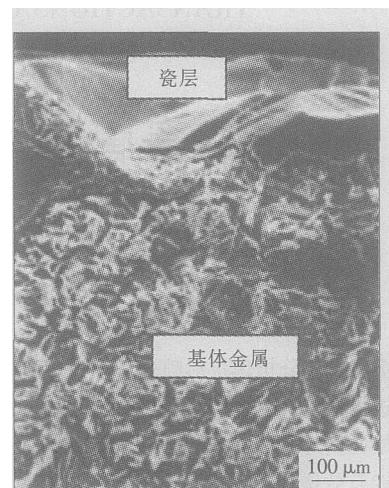


图 3 易脱瓷区脱瓷形貌(SEM)

Fig. 3 Morphology of enamel of easy doffing area

2.2 TIG 焊打底工艺

采用焊条电弧焊,由于根焊道焊完后,除热作用外,焊条药皮与釉料的作用也改变了瓷层的性质,并产生严重影响,使得焊缝底部瓷层极易脱落,裸露出焊缝金属,降低了管道的整体使用性能。而 TIG 焊具有电弧稳定性特别好的特点,试验中发现采用小电流、不填丝的 TIG 焊打底能够大大减小焊接对接头区瓷层的破坏。另一方面,采用焊条电弧焊时为了保证焊透并较好地反面成形一般留有较大间隙,而喷瓷管道瓷层的厚度一般为 0.3~0.6 mm,依靠焊口附近瓷层的自熔覆很难保证完全覆盖焊缝。要想使管口附近的瓷层能够覆盖焊缝,显然间隙越小越好,试验发现间隙小于 0.5 mm 时焊缝边缘的瓷层能很好地重熔、覆盖焊缝区。不填丝 TIG 焊可采用 0~0.5 mm 的间隙,确保瓷层能完全覆盖焊缝。为了保证采用较小的电流就能焊透,坡口的钝边厚度越小越好。试验中焊接试样采用 30°V 形坡口,没有钝边可以减小电流,从而减轻电弧对瓷层的破坏。焊接电流依次选择 30 A、50 A、110 A 和 150 A, 考察电流大小对接头区瓷层的防护效果。试验结果发现,焊接电流为 30 A 时,电流太小而在焊缝部分地区出现未焊透,而且焊接速度慢,效率低。当电流为 50 A 时焊缝成形良好,接头区背面有较好的防护瓷层,达到了自熔覆防护的目的。但由于热输入量小,重熔的瓷层很快冷却粘度急剧增大,气体不易逸出而形成了大量气泡,这些气泡势必会降低该处瓷层的耐蚀性。当电流增大到 110 A 时,虽然瓷层冷却速度减慢气泡减少,但热输入量过大导致焊缝中心处瓷层烧损、密着层消失、瓷层脱落、焊缝金属裸露。电流再增大到 150 A, 同样会导致瓷层脱落、焊缝金属裸露,虽然电流大降低了瓷层的冷却固化速

度,有利于气泡逸出,但由于热输入量过大产生了更多的气泡,这些气泡来不及逸出,焊后重熔区仍然有大量气泡存在。从瓷层自熔覆防护这一角度考虑,焊接电流应在 50 A 左右为宜。

采用焊前预热,能够减慢熔融瓷层冷却固化的速度,有利于气泡的逸出从而减少气泡,但并不能完全消除气泡。试验发现,预热温度为 300 °C 时依然存在一些气泡。

2.3 焊前管端预涂釉浆

采用以上的 TIG 焊打底工艺虽然能够很好地实现焊接接头的自熔覆防护,但由于喷瓷管道瓷层的厚度很薄,一般只有 0.3~0.6 mm,焊接时管端的瓷层重熔后一部分向焊缝流布,还有少量的瓷层会在焊接高温下烧损,因而焊后接头区的瓷层很薄,只有 0.1 mm 左右,瓷层太薄其耐蚀性得不到保证。如果在喷瓷管道制备时将管端内壁瓷层加厚,则会发现焊接时由于瓷层过厚瓷层内应力大,大部分瓷层还没有来得及重熔流动就崩瓷、脱落。

为了增加焊后接头区的瓷层厚度,提高其防护效果,采用了管端预涂釉浆的方法。将玻璃釉料和酒精按一定的配比用球磨机球磨成釉浆,焊接前将釉浆刷涂在焊接试块焊口附近约 10 mm 的范围内,示意图如图 4 所示。烘干后,釉浆成为粉尘,依靠粉尘间的结合强度附着在管端瓷层上。焊接时这些粉尘也会熔融并向焊缝区流动铺展,使得接头区的瓷层增厚,焊后接头区瓷层如图 5 所示。

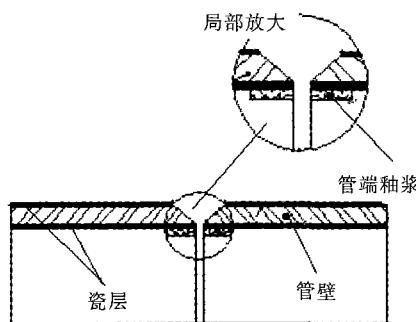


图 4 焊前管端预涂釉浆示意图

Fig.4 Brushing glaze slip onto end of pipe before welding

2.4 焊后接头区瓷层重熔处理

采用 TIG 焊打底、焊前管端预涂釉浆等措施能够很好的实现焊接接头的自熔覆目的,但仍然存在一些问题如重熔区的气泡、易脱瓷区的裂纹、瓷层与焊缝金属的密着性差等问题单靠调整焊接工艺参数和焊前处理无法从根本上解决。焊后采用氧-乙炔火焰从施焊面对接头区加热,在合适的温度下热量通过管壁传递给瓷层使接头区的瓷层重新软化,保温一定时间、缓慢冷却,这样一方面可以使气泡溢

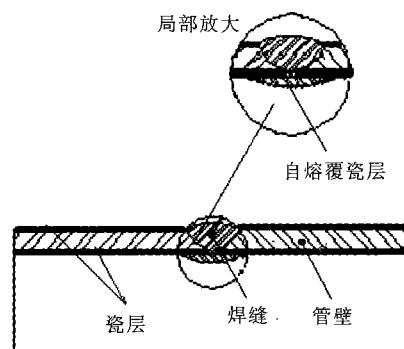


图 5 瓷层自熔覆示意图

Fig.5 Self-deposition of porcelain

出、裂纹愈合,并促进瓷层与焊缝金属的密着;另一方面可使部分依靠焊接热作用未熔化的管端预涂釉浆重新熔化,并使接头区瓷层重新软化、流布,瓷层更均匀致密。

后热重熔温度过低,瓷层不能软化,达不到效果;温度过高熔融瓷层与基体金属剧烈反应反而会产生更多的气泡,而且还会造成瓷层的烧损。由于瓷层的软化温度为 600~700 °C,而喷瓷管道的瓷层制备温度为 760 °C 左右,在该温度下能获得性能优良的瓷层而不会造成瓷层的烧损,故焊后重熔温度可确定为 700~800 °C。在喷瓷管道现场焊接时可采用环形管口加热器从管道外壁对焊口进行后热重熔处理,同时采用表面温度计从管道外壁对加热温度进行控制。

综合以上的工艺和措施,焊前在焊口附近预先刷涂釉浆,烘干后采用 TIG 焊打底,电流为 50 A,然后采用焊条电弧焊填充和盖面,电流为 110 A 左右。焊完后采用火焰加热对接头区进行重熔处理,温度控制在 700~800 °C,保温时间约 10 min。焊接完成后,观察接头处瓷层,发现焊口瓷层和刷涂的釉浆均很好地向焊缝区流布,在焊缝区形成了很好的保护层,焊后不用进行内补口。在接头区截取带瓷层的试样磨制金相(见图 6),接头区瓷层与管道原始内

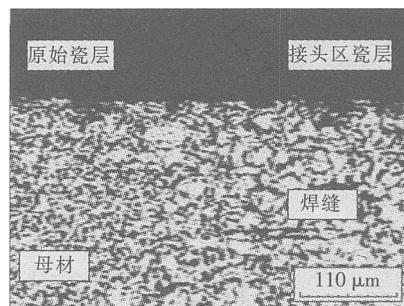


图 6 焊接接头区形貌

Fig.6 Morphology of welded joint

[下转第 55 页]

4 结 论

(1) 通过将转轮模型各部分定义成接触体的方法解决了具有复杂表面的叶片与空气之间的散热问题。

(2) 利用点连接的方法实现了焊接热源沿任意空间路径移动的加载问题。

(3) 转轮焊接应力场的模拟结果表明,焊接残余拉应力出现在叶片与上冠或叶片与下环接触区域附近的叶片上,并且在此区域出现焊接应力的峰值。同时结合有关研究人员对转轮工作应力的研究,对水轮机转轮的失效原因进行了分析。

参考文献:

- [1] 程良骏. 水轮机[M]. 北京: 机械工业出版社, 1982.
- [2] Courteau D. Performance and technical particulars of the double runner francis turbines[C]. Waterpower-Proceedings of the International Conference on Hydropower, 1995. 1491–1499.

[上接第 51 页]

壁瓷层形成一体,对接头区起到了防护作用,整个瓷层致密均匀,没有气泡、裂纹等缺陷。

3 结 论

(1) 喷瓷管道手工电弧焊焊接时,焊接热作用会使焊口处瓷层熔化、剥离、脱落,并产生裂纹、气泡等缺陷。采用 TIG 焊打底,在焊接电流合适的情况下不但会减小焊接热对瓷层的破坏作用,避免焊口处瓷层的剥离、脱落,而且能够使焊口附近的瓷层重熔并向焊缝流布、熔覆,在焊缝区形成保护层,对焊接接头起到自熔覆防护作用。

(2) 焊前管端预涂釉浆能有效增加接头区瓷层的厚度,提高瓷层的防护效果。

(3) 焊后采用火焰加热到 700~800 °C 对接头区进行重熔处理并缓慢冷却,接头区瓷层重新软化、流布。一方面可以消除接头区瓷层的缺陷如裂纹、气泡等,另一方面瓷层更均匀致密并促进了瓷层与焊缝金属的密着。

(4) 利用瓷层的自熔覆性能,采用焊前预涂釉浆、TIG 焊打底、焊后接头区重熔处理等措施能够有效解决喷瓷管道焊接接头的防护问题,焊后不用内

- [3] Baetz J P. The repair welding of ARSWIN runner[J]. Journal of Hydraulic Research, 1986, 24(3): 45–50.
- [4] Sotnikov A A. A russian turbine experience[J]. Water Power of Dam Construction, 1998, 50(5): 45–48.
- [5] 樊世英. 混流式水轮机转轮裂纹原因分析及预防措施[J]. 水力发电, 2002, 28(5): 38–41.
- [6] Mo Chuli, Qian Bainian, Gou Xuming, et al. The development of models about welding heat sourcess calculation[J]. Transactions of the China Welding Institution, 2001, 22(3): 93–96.
- [7] 莫春立, 钱面年, 国旭明, 等. 焊接热源计算模式的研究进展[J]. 焊接学报, 2001, 22(3): 93–96.
- [8] 沈炜良. 水轮机转轮的有限元计算及裂纹分析[J]. 广西大学学报, 2000, 25(3): 238–240.
- [9] 黄文. 水轮机转轮叶片的应力分布及其裂纹成因[J]. 实用测试技术, 1999, (3): 33–34.
- [10] 孙鸿秉. 岩滩水轮机转轮叶片裂纹原因探析[J]. 红水河, 1995, 15(3): 32–37.

作者简介: 姬书得,男,1977 年出生,博士研究生。主要从事水轮机转轮失效方面的研究,发表文章 8 篇。

Email: superjsd@hit.edu.cn

补口。

参考文献:

- [1] Odawara Osamu. Long ceramic-lined pipes with high resistance against corrosion, abrasion and thermal shock [J]. Mater. & Manuf. Proc., 1993, 8(2): 203–218.
- [2] Ashcroft I A, Derby B. Adhesion testing of glass-ceramic thick films on metal substrates[J]. J. Mater. Sci., 1993, 28(11): 2989–2998.
- [3] Wang Yong, Han Tao, Zhang Wenyue. Influene of thermal cycles on the coating corrosion resistance of sprayed porcelain pipe[J]. Transactions of the China Welding Institution, 2001, (22)6: 15–17.
- 王 勇, 韩 浩, 张文锐. 热循环对喷瓷管道瓷层耐蚀性的影响[J]. 焊接学报, 2001, 22(6): 15–17.
- [4] 邵文古, 王理泉. 金属–玻璃(釉)热喷复合防腐管道[P]. 中国专利: CN1051075A, 1991–05–01.
- [5] 王维东, 王 勇, 何艳玲, 等. 喷瓷管线接头焊后的涂层与基体的界面研究(I)[J]. 材料工程, 1998, (11): 28–29.

作者简介: 陈玉华,男,1979 年 5 月出生,博士研究生。主要从事金属表面工程和新材料连接技术方面的研究,发表论文 7 篇。

Email: ch.yu.hu@163.com

tral analysis system, the arc light spectral distribution in pulsed gas metal arc welding (P-GMAW) has been measured, and two filtering spectral windows suitable for the imaging of weld pool in P-GMAW have been proposed. The quality of pool images, taken with two kinds of filtering systems in which the middle wavelengths are 665 nm and 1 064 nm respectively, has been compared. A sequence of pool images in a single pulse have been taken and the results indicate that the end of base current period is the optimal imaging time. With the filtering system, whose middle wavelength is 665 nm, very clear weld pool images in base current period have been captured by imaging from up-rear direction of weld pool. Meanwhile, the imaging mechanism has been analyzed. A series of image processing programs have been developed, and accurate pool profile has been extracted.

Key words: pulsed gas metal arc welding; weld pool; visual monitoring; spectral analysis; image process

Bonding strength of double partial transient liquid phase bonding with $\text{Si}_3\text{N}_4/\text{Ti}/\text{Cu}/\text{Ni}/\text{Cu}/\text{Ti}/\text{Si}_3\text{N}_4$ ZOU Jia-sheng, XU Zhizong, ZHAO Qi-zhang, CHEN Zheng (East China Shipbuilding Institute, Zhenjiang 212003, Jiangsu, China). p41 - 44

Abstract: The influence of bonding parameters and testing temperature on bonding strength was studied under double partial transient liquid phase(PTLP) bonding with Si_3N_4 ceramic using $\text{Ti}/\text{Cu}/\text{Ni}$ interlayer. The results showed that the bonding strength at room temperature increases with second bonding temperature and second holding time, and bonding parameters have slight influence on thickness of reaction layer in $\text{Si}_3\text{N}_4/\text{Ti}/\text{Cu}/\text{Ni}$ interface of double PTLP bonding. The bonding strength was the highest at testing temperature 400 °C, and the bonding strength declined when the temperature continued to increase. But the high temperature strength had good stability if the temperature was less than 800 °C.

Key words: silicon nitride; double partial transient liquid phase bonding; bonding strength; high temperature strength

Microstructure of repairing welded joint of TA15 Ti alloy DU Xin¹, LIU Li-ming¹, SONG Gang¹, WANG Min², YANG Lei² (1. State Key Laboratory of Material Surface Modification by Laser, Ion, and Beams, Dalian University of Technology, Dalian 116024, China; 2. Shenyang Aircraft Corporation, Shenyang 110000, China). p45 - 48

Abstract: Microstructure characteristics of repairing welded joint of TA15 Ti alloy were analyzed by optics microscope, X-ray diffraction and electron probe microanalysis. The feasibility of Ti alloy multiple repairing welding was discussed. It was found that repairing welding was the process to form the new bead and heat-affected zone on the original bead. The interface quality of repairing welding bead and original bead is good and the defects, such as interphase reactants, air hole, crack and sediment, were not observed between the repairing welding layer and the original bead. Elements Ti, Al, V, Fe were distributed uniformly from repairing welding head to the base metal. Repairing welded joint structure in the room temperature was α -Ti. As repairing welding times increased, crystal grain grew up and dentate α -phase appeared. Micro-hardness in

repairing welding region tended to decrease to some degree. The results showed that repairing welding of TA15 Ti alloy was feasible.

Key words: TA15 Ti alloy; repairing welding; structure; argon arc welding

Protection of welded joints of sprayed porcelain pipe by self-deposition of enamel coating CHEN Yu-hua, WANG Yong, HAN Tao, DONG Li-xian (Department of Materials Science and Engineering, College of Mechanical and Electronic Engineering, University of Petroleum, Dongying 257061, Shandong, China). p49 - 51,55

Abstract: The effect of welding on the enamel of the welded joint of porcelain pipe was studied and a new method of self-deposition protection method was put forward to protect the welded joints of porcelain pipe. The results show that the enamel near the weld can remelt and flow to the weld and cover the weld metal when tungsten inert-gas (TIG) welding is used to backing weld with proper the current. Pre-brushing the enamel near the end of pipe before welding can add the thickness of the self-deposition enamel and improve the protection effect. Using flame to remelt the enamel on the welded joints after welding and cooling slowly can re-intensify the enamel and remove the cracks and air bubbles in the enamel. Using the methods of brushing enamel before welding, backing welding by TIG, filling by shield metal arc welding and remelting enamel on the welded joints by flame can effectively protect the welded joints of porcelain pipe without internal repairing after welding

Key words: corrosion resistance; sprayed porcelain pipe; welding; protection of welded joints; self-deposition property

Influence of blade stress state on invalidation of francis turbine runner JI Shu-de, FANG Hong-yuan, LIU Xue-song, MENG Qin-guo (National Key Laboratory of Advanced Welding Production Technology, Harbin Institute of Technology, Harbin 150001, China). p52 - 55

Abstract: Francis turbine runner's temperature field and stress field during welding processes are simulated, while considering thermal source's movement along any complicated spatial route and heat loss from blade to air. The evolution process of welding stress and the distribution of residual stress field after welding are obtained. The simulation result shows that maximal welding stress appears on the blade near the adjacent zone between blade and band or blade and crown. The invalidation reason of runner is explained, based on working stress distribution of runner.

Key words: welding; blade; stress field; invalidation

Experimental study on electro-slag weld of blast furnace steel using vibratory conditioning technology ZHU Zheng-qiang¹, CHEN Li-gong¹, RAO De-lin¹, NI Chun-zhen¹, LU Li-xiang², XU Li-xing² (1. Institute of Welding, Shanghai Jiaotong University, Shanghai 200030, China; 2. Shanghai Baosteel Metallurgical Construction Limited Corporation, Shanghai 201900, China). p56 - 58,63

Abstract: Vibratory conditioning technology was used in the electro-slag welding of blast furnace steel and mechanical properties of welded joint were measured. The results have proved that vibratory conditioning technology can effectively improve the comprehensive properties of welded joints. Especially, at the 0.6 acceleration of gravity vibratory state, the